Vibrational Dynamics of Terminal Acetylenes: III. Comparison of the Acetylenic C−H Stretch Intramolecular Vibrational-Energy Redistribution Rates in Ultracold Molecular Beams, Room-Temperature Gases, and Room-Temperature Dilute Solutions

Hyun S. Yoo, David A. McWhorter, and Brooks H. Pate*

Department of Chemistry, University of Virginia, McCormick Road, Charlottesville, Virginia 22904

Received: November 23, 2002; In Final Form: October 8, 2003

The population relaxation rate of the first excited state of the acetylenic C−H stretch is compared for a series of isolated and solvated terminal acetylenes. The isolated molecule relaxation rate for ultracold molecules is measured using high-resolution infrared spectroscopy in a molecular beam. These measurements use a microwave−infrared double-resonance technique to obtain rotationally resolved spectra that originate in the vibrational ground state. The relaxation rates in room-temperature gas and dilute CCl_4 solution (0.05 M) are measured using two-color transient absorption picosecond spectroscopy. Although the molecule-dependent contribution to the total relaxation rate in solution is proportional to the population relaxation rate measured for the isolated molecule under molecular-beam conditions, a large scale factor (27) is required to reach quantitative agreement. Part of the reason a large IVR scaling rate is observed can be attributed to the fact that the intramolecular vibrational-energy redistribution (IVR) dynamics of the terminal acetylenes occur on two distinct time scales. The faster time scale produces only partial redistribution of the excited-state population. The experimental limitations of high-resolution infrared spectroscopy make it likely that this time scale is undetected in the molecular-beam measurements. Instead, the slower time scale, which is about 5 times slower than the initial IVR rate, is more closely related to the IVR time scale measured using high-resolution molecular-beam infrared spectroscopy. In addition, a thermal factor is expected when comparisons are made between ultracold molecular-beam and room-temperature sample conditions. A comparison of the measured IVR rates under these two conditions suggests that the rate enhancement at room temperature is related to the average thermal energy of the molecule. Most of the molecules in this study have about the same thermal energy, and this energy provides a factor of 5 increase in the IVR rate over the value obtained under ultracold conditions. These two factors together explain the large increase in the isolated molecule rate when the molecular-beam IVR rate is compared to the solution-phase relaxation rate of the room-temperature sample.

Introduction

The vibrational dynamics of solvated molecules involve the interplay of purely intramolecular and solvent-induced relaxation processes. For a large molecule in solution, there are two pathways for the population relaxation of a coherently prepared excited state: an intramolecular pathway where the population is redistributed to other vibrational states of the molecule with the same total energy through anharmonic interactions (intramolecular vibrational-energy redistribution, IVR) and a solvent-relaxation pathway where the vibrational energy is removed from the molecule by a series of steps that lower the total vibrational energy (vibrational-energy relaxation, VER).[1−5] In the present series of papers, the vibrational dynamics of a set of terminal acetylenes are investigated in both gas and solution with the goal of understanding the relative contributions of IVR and VER and to determine whether the purely intramolecular vibrational dynamics are modified by solvent. This final paper in the series takes a unified look at the population relaxation rate of the first excited state of the acetylenic C−H stretch as the molecule moves from the ultracold, isolated environment of molecular beams to collision-free room-temperature gas conditions and finally to dilute solution at room temperature.

The previous papers compared IVR rates of gas-phase molecules with the total relaxation rate measured in solution for the acetylenic C−H stretch fundamental of terminal acetylenes at room temperature, where both rates were measured using time-domain pump−probe spectroscopy.[1,2] A good correlation observed between the IVR rates and the total relaxation rates in solution indicated a simple model for the interplay of intramolecular and intermolecular relaxation processes: the total solution rate is the sum of a molecule-dependent IVR rate and a solvent-induced VER rate that is common to all terminal acetylenes. In this study, we include frequency-domain molecular-beam measurements of the IVR rate of ultracold molecules. The molecular-beam experiments determine the state-specific IVR rate for single rotational levels of the acetylenic C−H stretch fundamental. Because the measurements are made using infrared−microwave double-resonance techniques, the high-resolution vibrational spectrum is unambiguously assigned to the C−H stretch fundamental without the possibility of the spectrum arising from a populated low-frequency normal mode (i.e., a hot band). By contrast, the room-temperature time-domain measurements contain contributions from almost all thermally populated vibrational levels and provide thermally averaged relaxation rates that could reasonably be expected to differ from the relaxation rate of the acetylenic C−H stretch fundamental.[6,7] Therefore, the extension of this study to include molecular-beam IVR rates has the potential to determine how thermal vibrational energy affects vibrational dynamics.

* Corresponding author. E-mail: bp2k@virginia.edu.

10.1021/jp0275443 CCC: $27.50
Published on Web 01/31/2004

TABLE 1: Lifetimes for the Acetylenic C−H Stretch in the Molecular Beam and in Room-Temperature CCl_4 Solution and Vibrational State Densities at 3330 cm^{-1}[a,b]

molecule	τ_{IVR-MB} (ps)	τ_{CCl4} (ps)	$\rho^{A1}{}_{3330\ cm^{-1}}$ ($/cm^{-1}$)	Q_{vib}	$\langle E_{vib}\rangle^c$ (cm^{-1})
H−C≡CCH_3		22(2.2)	0.66	1.81	197
H−C≡CCH_2F		36(3.6)	2.3	2.65	293
H−C≡CCH_2Cl		51(1.9)	4.4	3.11	339
H−C≡CCH_2Br		38(3.8)	5.1	3.57	370
H−C≡CCH_2CH_3	70(17)	7.8(0.8)	15	4.11	438
H−C≡CCH_2OH	400(150)	17(1.7)	19	3.68	398
H−C≡$CC(CH_3)$═CH_2	105(24)	3.6(0.5)	36	7.33	613
H−C≡CCH═$CHCH_3$(Z)	183(26)	5.5(0.6)	75	8.98	618
H−C≡CCH═$CHCH_3$(E)	83(16)	2.8(0.5)	84	9.59	641
H−C≡$CCHFCH_3$	133(20)	13(1.3)	120	6.36	574
H−C≡CCH_2CH_2F	1480(300)	23(2.3)	140	9.14	566
H−C≡CCH_2CH_2Cl	3480(700)	26(2.6)	160	13.1	631
H−C≡CCH_2CH_2Br	1990(400)	22(2.2)	210	17.3	673
H−C≡$CC(CH_3)_3$	210(30)	5.1(0.5)	700	25.5	1027
H−C≡CCH_2OCH_3	300(60)	15(1.5)	750	11.9	655
H−C≡$CCH_2CH_2CH_3$(g)	325(65)	9.0(0.9)	2400	13.0	707
H−C≡$CCH_2CH_2CH_3$(t)	1000(200)	13(1.3)	2400	16.1	728
H−C≡$CSi(CH_3)_3$	1835(250)	44(4.4)	21 000	340	1504

[a] State density with the same vibrational symmetry as that of the bright state, the acetylenic C−H stretch. [b] Also listed are the vibrational partition functions and the average vibrational energies at room temperature. [c] The average vibrational energy at room temperature that we report in this paper does not include the amount where the thermal energy is in the acetylenic C−H bend. As described in the previous paper,[1] because of the large anharmonicity (20 cm^{-1}), our picosecond pulse does not effectively excite the hot bands originating from the acetylenic C−H bend excitation at room temperature, so they are not likely to affect the IVR dynamics of the first excited state of the acetylenic C−H stretch.

Experimental Section

The experimental technique for the high-resolution IVR rate measurements has been previously described in detail.[8,9] Briefly, rotationally resolved infrared spectra are obtained with microwave−infrared double-resonance spectroscopy using an electric-resonance optothermal spectrometer (EROS).[10,11] The spectrometer consists of three chambers: the source chamber, flight chamber, and detector chamber. The sample is expanded from a pinhole nozzle (50 μm) in the source chamber, which contains microwave radiation ports and an infrared multipass assembly. The flight chamber includes a quadrupole state-focusing device. All spectroscopy is performed in the source chamber before the state-focusing device is overlapped with infrared and microwave radiation for double-resonance spectroscopy. The total beam flux is measured by a liquid-helium-cooled bolometer detector through the kinetic energy carried to the detector when the molecular beam reaches the bolometer detector.[12]

The vibrational relaxation rate measurements of solution-phase molecules using time-domain spectroscopy included in this study are identical to those described in the previous paper.[1] We have performed two-color picosecond transient absorption measurements where the total relaxation rate is measured through the anharmonically shifted $v = 1-v = 2$ absorption frequency. Solutions with a concentration of 0.05 M in carbon tetrachloride (CCl_4) were used at room temperature. The structural formulas for all of the molecules in this study are given in Table 1.

Results

IVR Rates from High-Resolution Infrared Spectroscopy. The intramolecular vibrational-energy redistribution rate of the first excited state of the acetylenic C−H stretch normal mode for an isolated molecule has been determined using high-resolution infrared spectroscopy in a molecular-beam spectrometer. The IVR rates for two of the molecules (($(CH_3)_3C-C\equiv CH$ and $(CH_3)_3Si-C\equiv CH$) were measured using a standard optothermal spectrometer in the previous work of Kerstel et al.[13] The other 16 IVR rate determinations are obtained from eigenstate-resolved spectra obtained using the EROS machine. Because these measurements are made using an infrared−microwave double-resonance technique, the IVR rates for single rotational levels of the acetylenic C−H stretch are obtained. In particular, the infrared spectrum is guaranteed to originate in a rotational level of the ground vibrational state. The IVR lifetimes obtained from high-resolution molecular-beam spectroscopy are presented in Table 1. This table also includes the vibrational state density at the energy of the first excited state of the acetylenic C−H stretch, the vibrational partition functions at room temperature, and the average thermal energy at 300 K. These three quantities are calculated in the harmonic limit using scaled ab initio vibrational frequencies calculated at the B3LYP/6-31g** level.[14] The reported state density is for the vibrational state with the same vibrational symmetry as that of the acetylenic C−H stretch (i.e., the vibrational state density available for anharmonic interactions).

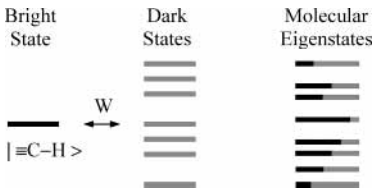

Figure 1. Standard model of IVR. One vibrational state, called the bright state, carries all of the oscillator strength to the higher-energy region. The bright state is coupled to the near-resonant vibrational dark states. The resulting molecular eigenstates can be written as linear combinations of the interacting bright and dark basis states. The bright-state oscillator strength is distributed among the eigenstates, and the intensity observed in the spectrum is proportional to the bright-state contribution to the molecular eigenstate. The dynamics of the bright-state population can be calculated from the survival probability. In general, the width of the intensity distribution reflects the initial population decay rate.

Frequency-domain measurements of the IVR rate are interpreted using the standard spectroscopic model shown in Figure 1.[15,16] The dynamics are described using the normal-mode vibrational states as a basis. In the spectral region of interest, a single vibrational state is assumed to carry all of the oscillator strength. In our measurements, this "bright state" is the first excited state of the acetylenic C−H stretch near 3330 cm^{-1} above the zero-point energy of the molecule. In this energy region, there will be other vibrational states that are the combination bands and overtones of the lower-frequency normal modes. These "dark states" are assumed to have no transition dipole strength from the ground state. The density of these dark states depends on the number and frequency distribution of the normal modes. Vibrational anharmonicity leads to interactions between the bright and dark states. The exact eigenstates of the molecular Hamiltonian can be represented in the normal-mode basis of bright and dark states. This vibrational-state mixing leads to a distribution of the bright-state transition intensity over several molecular eigenstates. The width of the intensity distribution reflects the time scale for population transfer from the normal-mode bright state (acetylenic C−H stretch) to the near-resonant dark states. This time scale can also be measured using time-domain techniques if the bandwidth of the excitation source is sufficiently broad to excite the full intensity profile coherently. Details of the analysis of eigenstate-resolved spectra are presented in Appendix A.

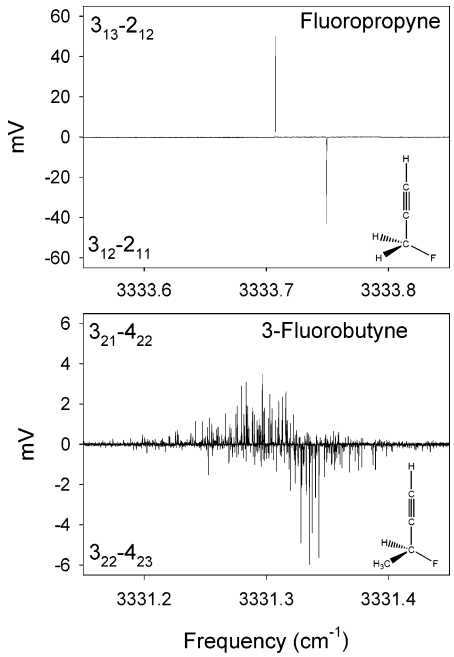

Figure 2. High-resolution infrared−microwave double-resonance spectra of fluoropropyne (top) and 3-fluorobutyne (bottom). The $2_{11}-2_{12}$ (standard asymmetric top notation: $J_{Ka,Kc}$) pure rotational transition of fluoropropyne at 1275.90 MHz is monitored for the IR-MW double-resonance spectroscopy of fluoropropyne. The $3_{13}-2_{12}$ and $3_{12}-2_{11}$ IR transitions are observed. Fluoropropyne ($\rho = 2.4$ states/cm^{-1}) lies below the IVR threshold vibrational state density (~10 states/cm^{-1}) and shows the lack of perturbation in the spectrum. For 3-fluorobutyne, the $4_{22}-4_{23}$ pure rotational transition at 1783.83 MHz is monitored, and the $3_{21}-4_{22}$ and $3_{22}-4_{23}$ IVR multiplets are obtained. The spectrum of 3-fluorobutyne ($\rho = 120$ states/cm^{-1}) shows extensive local perturbation resulting from IVR.

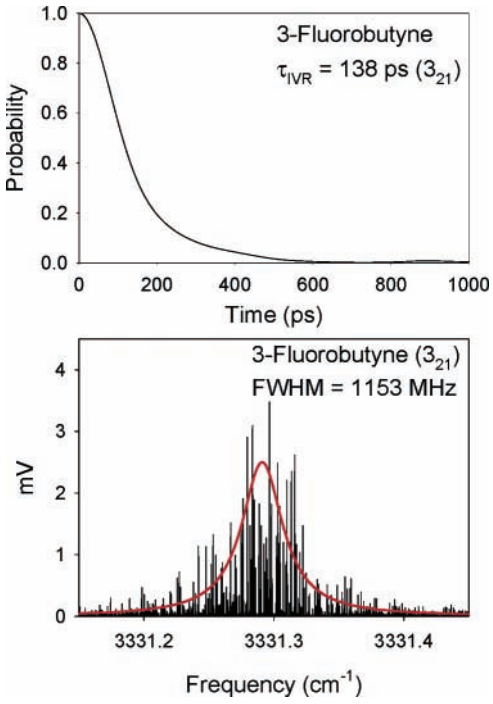

Figure 3. Survival probability for the 3_{21} rotational level of the 3-fluorobutyne acetylenic C−H stretch shown in the top panel. An IVR lifetime of 138 ps is calculated from the frequencies and intensities of the vibrational spectrum using eq A4. The Lorentzian line shape, derived from the calculated IVR lifetime of 138 ps, is also shown superimposed on the eigenstate-resolved spectum in the bottom panel.

To illustrate the analysis of the high-resolution spectra, the eigenstate-resolved infrared spectra for fluoropropyne and 3-fluorobutyne measured in double resonance with pure rotational transitions of the ground vibrational state are shown in Figure 2. These spectra illustrate the role that the total vibrational state density plays in IVR.[15,17] The state density of fluoropropyne at 3330 cm^{-1} is only 2.3 states/cm^{-1}. No local perturbations are observed in the spectrum of the 3_{13} or 3_{12} ($J_{Ka\ Kc}$: asymmetric top notation) rotational level of the excited state.[18] Several molecules in this study have "unperturbed" spectra like fluoropropyne. For these molecules, no IVR lifetime can be determined as indicated in Table 1. The spectrum of 3-fluorobutyne has a qualitatively different appearance. With the increase in state density to 120 states/cm^{-1}, the extensive local perturbations that result from IVR are now readily apparent. The survival probability for the 3_{21} rotational level of the acetylenic C−H stretch calculated using eq A4 is shown in Figure 3. A smooth decrease of the acetylenic C−H stretch population with an IVR lifetime of 138 ps is observed. This IVR lifetime can be used to determine the smooth Lorentzian line-shape contour that would describe a homogeneously broadened transition. For a lifetime of 138 ps, the full width of the Lorentzian line shape is 1153 MHz. The Lorentzian line shape derived from the survival probability lifetime is shown superimposed on the eigenstate-resolved spectrum in Figure 3. When the vibrational state density becomes very large such that individual eigenstates cannot be resolved in the high-resolution experiment, a smooth Lorentzian line shape can be expected. This limit is found for the two largest molecules in this study, $(CH_3)_3C-C\equiv CH$ and $(CH_3)_3Si-C\equiv CH$, and the IVR rates in Table 1 were determined from the line width of the Lorentzian line shape.[13]

The high-resolution molecular-beam spectroscopy measurements of the IVR rate are rotationally resolved. Therefore, for each molecule several IVR lifetimes are obtained. For the molecules in this study, we found no significant increase in the IVR rate with increasing total angular momentum (J). This result indicates that rotationally mediated intramolecular interactions, such as Coriolis coupling, are weak compared to anharmonic interactions. However, there is still variation in the IVR rates for different rotational levels. The IVR lifetimes listed in Table 1 are the average over all measured rotational levels. The uncertainty we report for the molecular-beam rate measurements reflects the spread of rates from the different rotationally resolved measurements. This "uncertainty" estimate derived from the rotational dependence of the IVR rate does not reflect any systematic errors in the rate determination.

Vibrational-Energy Relaxation Measurements in Dilute CCl_4 Solution. In addition to 10 terminal acetylenes with relatively low boiling points that allowed us to study room-temperature gas-phase IVR dynamics using the time-domain technique, 9 more molecules are included in this study. The IVR lifetime of the acetylenic C−H stretch in dilute CCl_4 solution is reported in Table 1 for all of the molecules in this larger study. Methylbutyne, included in the first two papers of this series, is omitted from this study because the low sensitivity precluded the determination of an IVR rate by the molecular-beam measurement. Propargyl bromide and propargyl alcohol are added as molecules with a single, stable conformation, and the interpretation of the absorption signal for these two molecules is identical to the one described in the previous paper.[1]

Also included in the present study are *E*- and *Z*-pentenyne, whose synthesis produces an equal mixture of the two conform-

ers. Distillation with a 1 m column can achieve reasonable separation of the structural isomers. For this study, lifetime measurements were made on a sample with a 2:1 mixture of E and Z isomers and on a sample that was a 1:2 mixture. The relative composition of the sample was determined by NMR spectroscopy. For these measurements, the decay curve was fit using a biexponential decay. For the 2:1 mixture, an unconstrained fit yielded lifetimes of 2.7 and 6.1 ps with an amplitude ratio of 2.3:1, in good agreement with the known isomer composition ratio. For the 1:2 mixture, the unconstrained biexponential fit returned lifetimes of 3.8 and 7.1 ps with amplitude ratios of 1:4.5. A second fit of the 1:2 mixture with the amplitude constrained to the 1:2 ratio gave lifetimes of 2.8 and 4.8 ps. These values agree well with the fit results of the 2:1 mixture. The lifetimes reported in Table 1 use the mean value of the lifetimes obtained from the two different samples.

For molecules with two stable conformations, such as 1-pentyne, the fitting procedure is complicated by the fact that the relative conformer populations are not known in solution. For these molecules, the data was fit to a biexponential decay with unconstrained amplitudes for the two components. Only 1-pentyne required a second decay component. The results for the biexponential fit of 1-pentyne are lifetime components of 9.0 and 12.9 ps and an amplitude ratio of 2.3:1. The results for the terminal acetylenes with conformations agree with predictions from ab initio calculations, molecular-beam measurements, and low-resolution room-temperature IR studies (where available). For example, ab initio calculations predict that the gauche conformer of 1-pentyne is only 98 cm^{-1} lower in energy than the trans conformer.[14] In the molecular-beam measurements, the infrared spectrum of both conformers is observed.[19,20] Therefore, we expect to observe biexponential decay data for 1-pentyne with a gauche/trans ratio of about 2:1. (There are two enantiomers for the gauche conformation.) Therefore, we assign the relaxation lifetimes of 9.0 and 12.9 ps to the gauche and trans conformations, respectively.

For the remaining terminal acetylenes with two conformations, single-exponential decay is observed, suggesting that only a single conformer contributes (or possibly that both conformers have the same lifetime). Ab initio calculations for methylpropargyl ether, 4-fluorobutyne,[21] 4-chlorobutyne, and 4-bromobutyne give energy differences between the conformers of 263, 426, 508, and 516 cm^{-1} respectively. The trans conformer is more stable for the halobutynes, but the gauche conformer is more stable for methylpropargyl ether. The molecular-beam infrared spectra for these molecules show only one vibrational band in the acetylenic C−H stretch region that is unambiguously assigned to the predicted low-energy conformer through microwave−infrared double-resonance spectroscopy. Because conformer populations in molecular beams usually reflect the room-temperature distribution, these measurements suggest that a single conformation dominates the room-temperature sample.[22,23] On the basis of the ab initio calculations and experimental evidence in the molecular-beam studies, the population relaxation lifetimes for methylpropargyl ether, 4-fluorobutyne, 4-chlorobutyne, and 4-bromobutyne are assigned to the lowest-energy conformation.

Discussion

One issue we are interested in for this study is whether the IVR rates of ultracold molecules measured by high-resolution molecular-beam spectroscopy reflect dynamics that are important in the vibrational relaxation process of room-temperature solutions. Using the same techniques employed in the previous papers,[1,2] we directly compare the IVR rate from frequency-domain molecular-beam spectroscopy to the total relaxation rate in dilute CCl_4 solution measured using two-color transient absorption spectroscopy in Figure 4. The plot of the 18 rate measurements in dilute CCl_4 solution and in the molecular beam is shown in Figure 4. The correlation of the total solution rate and cold-molecule IVR rate is good with two apparent outliers: 1-butyne and 3-fluorobutyne. Compared to the other molecules in the study, it appears that the IVR rate is faster than expected (or, equivalently, the solution rate is slower than expected) for 1-butyne and 3-fluorobutyne.

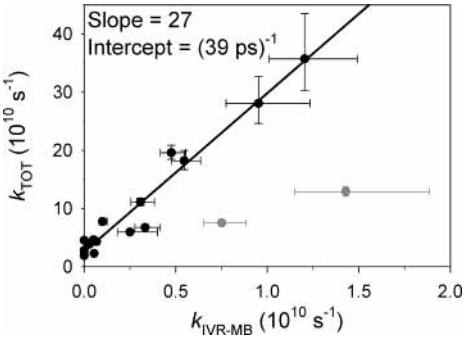

Figure 4. Total vibrational-energy relaxation rate in room-temperature CCl_4 solution (k_{TOT}) plotted against the molecular-beam IVR rate (k_{IVR-MB}). With the exception of 1-butyne and 3-fluorobutyne (shown in gray), the plot shows a correlation between the solution rate and the molecular-beam IVR rate. The linear regression (omitting the two outliers) shows a large scale factor of 27(1.6) (the slope) between the two rates. The linear relationship implies that the solvent contribution is constant throughout the series of molecules. The VER contribution to the total relaxation rate in CCl_4 solution is $(39(11)\ ps)^{-1}$ (the intercept of the regression result). The molecular-beam IVR lifetime uncertainty is determined from the standard deviation of the lifetimes for different rotational levels of the acetylenic C−H stretch. The solution-phase uncertainty is determined by the standard deviation of several measurements of the decay rate.

To analyze the results of isolated and solvated terminal acetylenes, we use the simple model for the total relaxation rate measured in solution (Figure 1 of ref 1). The total relaxation rate in solution[1,2] is

$$k_{TOT} = k_{VER} + k_{IVR} \quad (1)$$

As explained in the previous paper[1], the IVR contribution to the total relaxation rate is molecule-dependent whereas the VER contribution was found to be approximately the same for all terminal acetylenes in a given solvent. If the IVR rate measured for vibrationally and rotationally cold molecules in the molecular-beam studies is the same as the IVR rate for a room-temperature sample, then a plot of room-temperature solution rates and molecular-beam IVR rates would have a slope of 1.[1,2] However, in this case we instead observe a large slope for the correlation. The total relaxation rate in solution can be related to the ultracold-molecule IVR rate using the following modified expression

$$k_{TOT} = k_{VER} + c\, k_{IVR-MB} \quad (2)$$

where k_{IVR-MB} is the molecular-beam rate. Linear regression of the plot in Figure 4 gives an IVR scale factor of 27(1.6) and a VER contribution to the total relaxation rate of 39(11) ps when 1-butyne and 3-fluorobutyne are omitted. (The values with both of these molecules included are 17(3.4) and 25(12), respectively.) This value of the VER contribution to the total relaxation rate (39(11)) is the same within uncertainties as the value reported in the previous paper (67(22) ps) using a smaller data

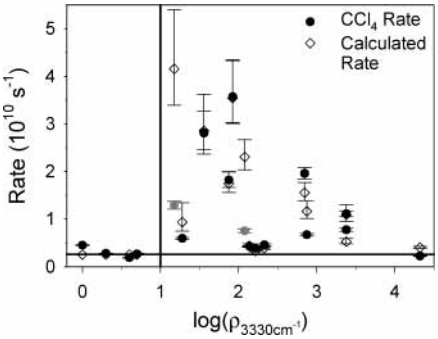

Figure 5. Measured solution rate (●) and calculated rate using eq 2 (◇), plotted as a function of the vibrational state density at 3330 cm^{-1}. The horizontal line is the solvent-induced VER rate in dilute CCl_4 solution, which is $(39\ ps)^{-1}$ and indicated as the intercept of the regression line in Figure 4. The vertical line shows the IVR threshold vibrational state density of 10 states/cm^{-1}. The solution relaxation rate tracks the scaled molecular-beam IVR rate, showing that the intramolecular dynamics are the major source of molecule-by-molecule variation in the solution rate. See Table 1 for the molecules in this plot.

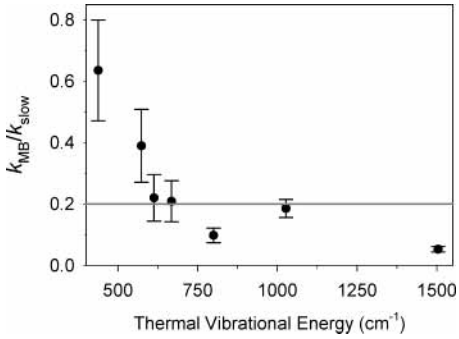

Figure 6. Thermal effect on IVR rates between samples at two different thermal conditions (cold molecular beam vs room-temperature gas). As the average thermal vibrational energy increases, the ratio of the molecular-beam IVR rate and the slower IVR time scale of the room-temperature gas-phase measurement approaches a value of about $^1/_5$, which is shown as the horizontal reference line.

set.[1] As discussed in the previous papers, the observed linear relation indicates that the solvent contribution to the total relaxation rate in solution is the same for all terminal acetylenes.[1,2] Reasons for the observation of the large scale factor and the two apparent outliers are discussed below.

The similarity between the total relaxation rate in solution and the molecular-beam IVR rate is further illustrated in Figure 5. In this figure, the measured solution relaxation rate and the relaxation rate predicted by the best fit to eq 2 are shown as a function of the vibrational state density at 3330 cm^{-1} (given in Table 1). Because the model (eq 2) includes a constant VER contribution for all terminal acetylenes, the variation in the solution relaxation rates is entirely attributed to the IVR process. The IVR rates for the terminal acetylenes span a wide dynamic range and are uncorrelated with the total vibrational state density. The combination of these two features produces a distinctive pattern of the relaxation rate when plotted against the vibrational state density. As seen in Figure 5, the pattern obtained from the ultracold molecular-beam measurements accounts for the variation in the room-temperature solutions.

Although a strong correlation is found between the solution rate and the molecular-beam IVR rate, the large IVR scale factor ($c = 27$) still remains to be explained. We believe that this result is caused by the unique features of IVR in terminal acetylenes and by limitations of the high-resolution spectroscopy technique. Using picosecond transient absorption spectroscopy on room-temperature gases, we were able to detect an initial IVR step that produced a partial decay of the acetylenic C−H stretch population.[1] Two-color transient absorption spectroscopy was used to show that this fast process involved population transfer to near-resonant normal-mode states that contain 2 quanta of acetylenic C−H bend excitation.[2] These results indicate a hierarchical energy flow that can be described using tier models for IVR.[24−27] In the first stage, restricted IVR through an acetylenic C−H stretch−bend interaction populates a few of the near-resonant bath states. On a slower time scale, the population is more completely redistributed to the high-density vibrational bath. This second step would lead to extensive fragmentation of the high-resolution spectrum as shown in Figure 3. For the molecules in our time-domain study, this second stage of more complete redistribution was found to be about 5 times slower than the initial IVR step.

The connection between frequency-domain spectroscopy and the excited-state dynamics was described in detail in the previous work. (See Appendix C of ref 1.) To detect the frequency-domain features that correspond to the fast initial IVR process, high sensitivity and long measurement times would be required. A likely scenario is that the high-resolution spectrum would measure only the transitions in the frequency range around the strong central feature. This result can come from either insufficient spectrometer sensitivity or experimenter bias for scanning only the regions where intense transitions occur. As illustrated in Figure A14 of ref 1, if the high-resolution spectrum is measured only in the region of the main spectral feature, then the second, slower time scale of the vibrational dynamics is observed. Our experience with the molecular-beam spectrometer used to make the ultracold IVR measurements suggests that the fastest measurable IVR rates are about $(30\ ps)^{-1}$.

With these considerations in mind, we believe that a large part of the scaling observed between ultracold IVR rates and total solution-phase relaxation rates comes from the fact that different stages of the terminal acetylene IVR process are detected in the two measurements. The discussion above suggests that the molecular-beam spectrometer is biased toward measuring the slow time scale of IVR. However, in the previous work we found that the total relaxation rate in solution correlated with the initial IVR rate of room-temperature terminal acetylenes. The fact that correlation is observed in Figure 4 suggests that the ratio of the fast and slow IVR rates (a ratio of 5 based on our results) is the same for most terminal acetylenes.

The remaining scale factor, which is about 5, can be attributed to the IVR enhancement caused by the population of higher-energy vibrational and rotational states in the room-temperature sample. With the availability of both ultracold and room-temperature IVR rates, we can compare the rate enhancement to the average thermal energy. This comparison is made for the terminal acetylenes in Figure 6. On the basis of the previous discussion, we believe that the molecular-beam IVR should be compared to the slower stage of IVR found in the room-temperature measurement. With the limited data set available, we observe a systematic increase in the IVR rate enhancement with thermal vibrational energy. To further test whether the thermal energy increases the IVR rate, we have performed temperature-dependent two-color transient absorption measurements. The temperature-dependent excited-state population decay is shown for butyne and *tert*-butylacetylene (TBA) in Figure 7. The main effect of raising the temperature is to decrease the lifetime of the second stage of IVR (complete redistribution to the near-resonant bath). Butyne, which is small and has fewer low-frequency vibrational modes than TBA, is less susceptible to temperature increases.

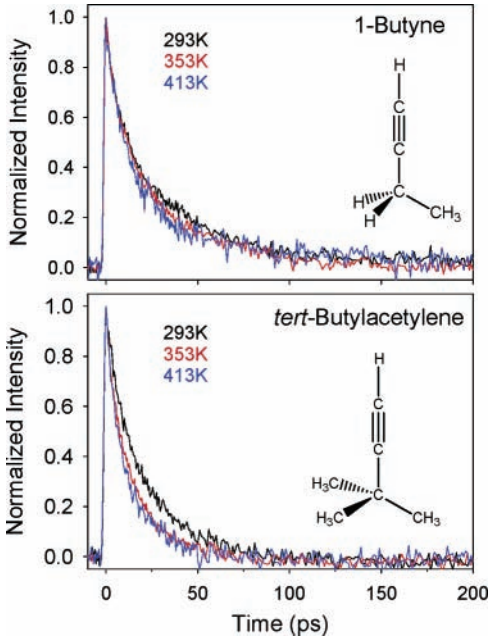

Figure 7. Temperature-dependent IVR rate change shown with transient absorption spectra taken at three different temperatures (293, 353, 413 K) for butyne and TBA. This result shows the effect of the sample temperature (average vibrational energy of a molecule) on the IVR rate. The IVR rate of larger molecule (TBA) with higher initial thermal vibrational energy is more readily affected by the temperature change than that of smaller molecule (butyne).

The results of Figure 6 suggest that the ratio of the room-temperature and ultracold IVR rates should be about a factor of 5 for most of the molecules in this study. That is, most of the molecules that have molecular-beam IVR rate determinations have thermal vibrational energies in the range of 550−750 cm^{-1} (Table 1). In general, we find that the molecules below the predicted slope (indicating less IVR enhancement) are the smaller molecules that carry less thermal vibrational energy and larger molecules with higher initial thermal energy are generally found above the predicted line (more IVR enhancement). This result provides a possible explanation for the "outlier" behavior of butyne and 3-fluorobutyne shown in Figure 4.[28] These two molecules are among the smallest to show IVR and have low initial thermal vibrational energy that provides little enhancement of the IVR rate compared to the beam measurement. The thermal enhancement factor we have determined for the terminal acetylenes is consistent with results for alcohols. For example, the few molecular-beam measurements of the IVR rate of the O−H stretch of alcohols are only 2−5 times slower than the total relaxation rate in solution (ethanol: 30−60 ps for the isolated molecule,[29] 13 ps in solution;[30] propargyl alcohol: 30−60 ps (isolated),[8] 14 ps (solution)[31]).

In summary, we attribute the unusual correlation of molecular-beam IVR rates and solution-phase relaxation rates (i.e., correlated but with a large scale factor) to two different effects. A factor of 5 can be assigned to the fact that the measurements detect different stages of IVR. However, the IVR rates of the stages occur in a 5:1 ratio that is about the same for the terminal acetylenes. Another factor of 5 (making a total scale factor of 25) is attributed to the rate enhancement of the second, slower IVR process caused by thermal excitation in the low-frequency normal modes. Again, for the correlation to persist, all terminal acetylenes would need to have the same scale factor. We believe this occurs because most of the molecules in the study have about the same thermal energy. Furthermore, if only vibrational modes directly coupled to the acetylenic C−H stretch strongly affect the IVR rate of the acetylenic C−H stretch, then a constant scale factor is appropriate because the normal-mode frequencies associated with the acetylenic chromophore are conserved for the terminal acetylenes. Therefore, the thermal population of these "important" modes is identical for all molecules and largely independent of the identity of the substituent group. These conclusions are illustrated by comparing the different measurements used in this study for 1-butyne in Figure 8. This molecule is a good choice for this analysis because it is the smallest molecule with fast IVR. At room temperature, ~25% of the molecules are in the ground vibrational state (Table 1). Therefore, the slow component of the gas-phase relaxation will contain a large contribution from the same vibrational state measured in the molecular-beam experiments. In the first part of Figure 8, the fit of the gas-phase spectrum to a biexponential form is shown. The two time constants from this fit are then compared to the solution-phase measurement (using the fast component of the gas-phase dynamics) and molecular-beam measurement (using the slow component). Excellent agreement with both the solution and molecular-beam results is achieved.

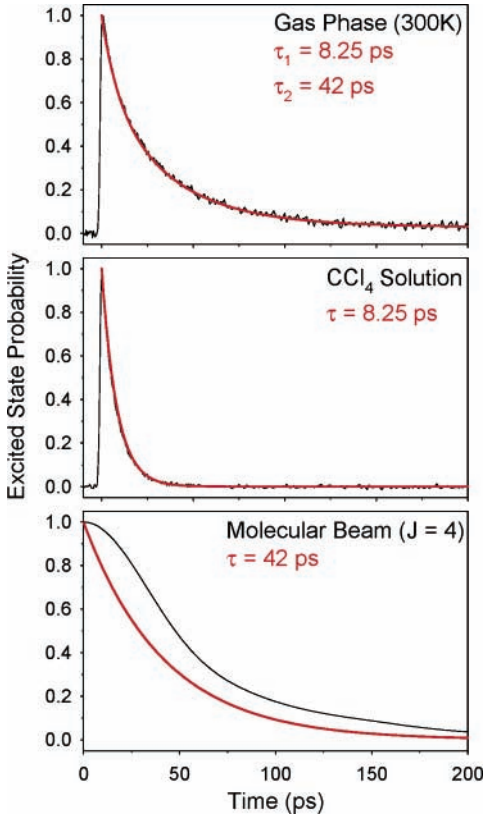

Figure 8. Application of the tier-model analysis to 1-butyne. The room-temperature gas-phase spectrum is shown with a biexponential fit result in the top panel. The fast time constant (8.25 ps) is compared to the CCl_4 solution measurement, and the second time constant (42 ps) is compared to the molecular-beam measurement. The tier-model analysis of the gas-phase result is in good agreement with both the solution and molecular-beam results.

Conclusions

The experiments reported in this set of three papers represent the first systematic study designed to uncover the roles that the purely intramolecular vibrational dynamics and solvent-induced vibrational-energy relaxation play in the total solution-phase vibrational relaxation process. A key component of this study has been the application of ultrafast vibrational spectroscopy techniques to room-temperature gas-phase samples. These experiments provided new insight into the IVR dynamics of

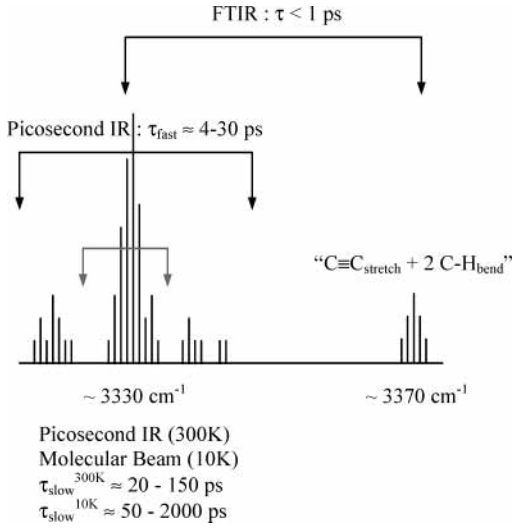

Figure 9. Schematic picture of the three different time scales investigated in this study. The fastest process is the population transfer from the acetylenic C−H stretch to a specific vibrational state—the combination band of the C≡C stretch and 2C−H bend. For most terminal acetylenes, this process is fast (<1 ps), but the population transfer is small (~5%) in this step. The main spectral feature, which we call the acetylenic C−H stretch, controls the subsequent dynamics. The second process is the energy redistribution to the vibrational states with C−H bend overtone excitation, which happens on a time scale of 4−30 ps. The final step is the energy redistribution to the rest of the vibrational modes of the molecule. As shown in our study, the final time scale is about 5 times slower than the second process (fast redistribution into the bend overtone states in room-temperature samples). The high-resolution molecular-beam spectroscopy (vibrationally cold molecules) also measures the dynamics of the final relaxation process. The redistribution rate of the final step in a cold molecule is about a factor of 5 slower than the one in a room-temperature sample, which is attributed to the thermal population of higher-energy vibrational and rotational states.

terminal acetylenes. In this section, the conclusions reached in the full study are summarized.

By using a combination of vibrational spectroscopy techniques (FTIR spectroscopy, picosecond infrared spectroscopy, and high-resolution molecular-beam infrared spectroscopy), a consistent picture of the isolated-molecule intramolecular dynamics of the first excited state of the acetylenic C−H stretch emerges. A schematic picture of the coupling hierarchies for the isolated molecule and their relationship to the different experimental techniques is illustrated in Figure 9. Although it has not been the focus of these papers, the initial redistribution event for most of the terminal acetylenes is a fast (<1 ps) population redistribution to a specific vibrational state, with the combination band composed of the C≡C stretch + 2C−H bend. These dynamics are evident in the FTIR spectra of both gas and solution samples. (See Appendix A of ref 1.) For most terminal acetylenes, the population transfer from this step is small (~5%). The important exception is molecules such as methylbutenyne, where conjugation of the acetylene with a C=C bond brings this state into almost exact resonance. In this case, a fast coherent energy transfer of large amplitude occurs between the two states. The two-level population oscillation that occurs in this situation is evident in the time-resolved transient absorption spectra of methylbutenyne shown in the previous papers.[1,2]

The second stage of the IVR dynamics has been revealed by picosecond transient absorption spectroscopy. The second time scale reflects population redistribution to near-resonant vibrational states with 2 quanta of the C−H bend. This process occurs on a time scale of 4−30 ps and is molecule-dependent. For the molecules where we have observed this fast step, about $^1/_3$ of the C−H stretch population is transferred in this stage of the isolated-molecule dynamics. In the final relaxation step, the vibrational energy is redistributed to the rest of the vibrational modes of the molecule. This final time scale is about a factor of 5 slower than the fast redistribution into the bend overtone states in room-temperature samples. This final relaxation process is also measured for rotationally and vibrationally cold molecules by high-resolution molecular-beam spectroscopy. By making IVR measurements under room-temperature and ultracold conditions, it becomes possible to assess the importance of thermal vibrational energy on the acetylenic C−H stretch dynamics. This analysis has been the focus of the present paper. Compared to the room-temperature measurements, the redistribution rate in the cold sample is about 5 times slower for most of the molecules in this study.

The major conclusion of this series of papers is that a simple model for the competition between IVR and VER quantitatively accounts for all of the measurements in this study. (For example, see Figure 8 of ref 2 where 50 measurements are shown with predictions using this model.) In this model, the total solution-phase relaxation rate of the terminal acetylenes is the sum of the molecule-dependent IVR rate and a molecule-independent VER rate. We find that the molecule-by-molecule variation in the solution-phase relaxation rates for the two stages of population relaxation can be attributed to the purely intramolecular dynamics. The characteristic pattern of these solution-phase vibrational relaxation rates is already evident in the IVR rates measured for isolated, ultracold molecules using high-resolution molecular-beam spectroscopy (Figure 5).

The second interesting feature of this model is that a single VER rate common to all terminal acetylenes is sufficient to reproduce the total solution-phase relaxation rates quantitatively in all cases. This "universal" VER rate for the terminal acetylenes shows some variation with the solvent (VER lifetimes of 40−70 ps for the first stage of IVR detected in the picosecond measurements). Also, the solvent contribution to the total solution-phase relaxation rate is different for the two stages of IVR detected in the transient absorption measurements. The molecule independence of the VER rate contribution suggests that solvent-induced vibrational-energy relaxation is a local process that allows all terminal acetylenes to behave the same way. We believe that this behavior is related to the commonality of the vibrational force-field of the acetylene chromophore, a property that makes these systems attractive for theoretical calculations.[32−34] Because we have been able to isolate the VER rates by properly accounting for the IVR dynamics, the terminal acetylene data set should provide a good test for current theoretical techniques used to calculate VER rates.[35−37]

Acknowledgment. We thank John Keske and Frances Rees for their help with the terminal acetylene sample set. This work was supported by the Chemistry Division of the National Science Foundation (CHE-0078825) and the Optical Sciences and Engineering Division of the National Science Foundation. Additional support for this work came from the SELIM Program and the AEP Program at the University of Virginia.

Appendix A: Obtaining IVR Rates from Eigenstate-Resolved Vibrational Spectra

The IVR rate of $v = 1$ of the acetylenic C−H stretch is obtained from the eigenstate-resolved infrared spectrum through the calculation of the survival probability.[15,16] As illustrated in Figure 1, the manifestation of IVR in the frequency-resolved spectrum is the presence of extensive local perturbations to the spectrum. Each molecular eigenstate (ϕ_i) can be represented in

the zeroth-order normal-mode basis set

$$|\phi_i\rangle = c_{bi}|\equiv \mathrm{CH}\rangle + \sum_j c_{dj_i}|\mathrm{dark}_j\rangle \quad \text{(A1)}$$

In this expression, the expansion coefficient for the acetylenic C−H stretch (c_b, where b denotes that this is the bright state) is separated from the coefficients for all of the other near-resonant overtone and combination band states (c_{dj}; the jth dark state). This separation is physically important because only the acetylenic C−H stretch normal-mode state carries appreciable oscillator strength from the ground state (i.e., the acetylenic C−H stretch is the bright state in this energy region). The intensity of an infrared transition to a single eigenstate is related to the acetylenic C−H stretch contribution

$$I_i \propto |c_{bi}|^2 \quad \text{(A2)}$$

Each molecular eigenstate is a stationary state of the full molecular Hamiltonian. Eigenstate-resolved excitation does not lead to any subsequent dynamics. Eigenstate-resolved excitation does not produce the acetylenic C−H stretch motion but instead results in a complicated vibrational motion that involves the motion of all of the nuclei.

Intramolecular dynamics result from the preparation of a superposition state through the coherent excitation of multiple molecular eigenstates. If a laser pulse with a short duration is used to excite the spectrum, then the prepared state will be

$$|\Psi(0)\rangle = \sum_i c_{bi}|\phi_i\rangle = |\equiv \mathrm{CH}\rangle \quad \text{(A3)}$$

This result assumes that the acetylenic C−H stretch is the only infrared-active vibration in the energy range covered by the laser pulse and that the laser pulse duration is much shorter than the population relaxation rate of the acetylenic C−H stretch. As indicated in eq A3, this initial state resulting from idealized short-pulse excitation is simply the acetylenic C−H stretch normal-mode basis state. This zeroth-order state is not an eigenstate of the full molecular Hamiltonian and will therefore undergo nontrivial time evolution. The survival probability of the acetylenic C−H stretch can be calculated in the molecular eigenstate basis

$$P(t) = |\langle\Psi(0)|\Psi(t)\rangle|^2 = \sum_i |c_{bi}|^4 + \sum_{i>j} |c_{bi}|^2|c_{bj}|^2 \cos\left(\frac{E_j - E_i}{\hbar}t\right) \quad \text{(A4)}$$

This result shows that the survival probability can be obtained from the frequency (to obtain $E_j - E_i$) and relative intensity ($|c_{bi}|^2$) information in the high-resolution, eigenstate-resolved spectrum. In general, the survival probability has an approximately exponential decay to the long-time limit called the dilution factor (ϕ_d)

$$\phi_d = \sum_i |c_{bi}|^4 \quad \text{(A5)}$$

The dilution factor can be related to the effective number of states participating in the IVR dynamics

$$N_{\mathrm{eff}} = \frac{1}{\phi_d} \quad \text{(A6)}$$

The IVR lifetimes for the acetylenic C−H stretch listed in Table 1 are defined as the time it takes for the probability to decay to $^1/_e$ of the long-time, or equilibrium, limit (ϕ_d).

References and Notes

(1) Yoo, H. S.; DeWitt, M. J.; Pate, B. H. *J. Phys. Chem. A* **2004**, *108*, 1348.

(2) Yoo, H. S.; DeWitt, M. J.; Pate, B. H. *J. Phys. Chem. A* **2004**, *108*, 1365.

(3) Bingemann, D.; King, A. M.; Crim, F. F. *J. Chem. Phys.* **2000**, *113*, 5018.

(4) Egorov, S. A.; Skinner, J. L. *J. Chem. Phys.* **2000**, *112*, 275.

(5) Assmann, J.; Charvat, A.; Schwarzer, D.; Kappel, C.; Luther, K.; Abel, B. *J. Phys. Chem. A* **2002**, *106*, 5197.

(6) von Puttkamer, K.; Dübal, H.-R.; Quack, M. *Faraday Discuss. Chem. Soc.* **1983**, *75*, 197.

(7) Bagratashvili, V. N.; Kuzmin, M. V.; Letokhov, V. S.; Stuchebrukhov, A. A. *Chem. Phys.* **1985**, *97*, 13.

(8) Hudspeth, E.; McWhorter, D. A.; Pate, B. H. *J. Chem. Phys.* **1998**, *109*, 4316.

(9) Cupp, S.; Lee, C. Y.; McWhorter, D.; Pate, B. H. *J. Chem. Phys.* **1998**, *109*, 4302.

(10) Fraser, G. T.; Pine, A. S. *J. Chem. Phys.* **1989**, *91*, 637.

(11) Lee, C. Y.; Pate, B. H. *Chem. Phys. Lett.* **1998**, *284*, 369.

(12) Gough, T. E.; Miller, R. E.; Scoles, G. *Appl. Phys. Lett.* **1977**, *30*, 338.

(13) Kerstel, E. R. Th.; Lehmann, K. K.; Mentel, T. F.; Pate, B. H.; Scoles, G. *J. Phys. Chem.* **1991**, *95*, 8282.

(14) The vibrational frequencies were calculated at the B3LYP/6-31g** level using the Gaussian 98 program. Frisch, M. J.; Trucks, G. W.; Schlegel, H. B.; Scuseria, G. E.; Robb, M. A.; Cheeseman, J. R.; Zakrzewski, V. G.; Montgomery, J. A., Jr.; Stratmann, R. E.; Burant, J. C.; Dapprich, S.; Millam, J. M.; Daniels, A. D.; Kudin, K. N.; Strain, M. C.; Farkas, O.; Tomasi, J.; Barone, V.; Cossi, M.; Cammi, R.; Mennucci, B.; Pomelli, C.; Adamo, C.; Clifford, S.; Ochterski, J.; Petersson, G. A.; Ayala, P. Y.; Cui, Q.; Morokuma, K.; Malick, D. K.; Rabuck, A. D.; Raghavachari, K.; Foresman, J. B.; Cioslowski, J.; Ortiz, J. V.; Stefanov, B. B.; Liu, G.; Liashenko, A.; Piskorz, P.; Komaromi, I.; Gomperts, R.; Martin, R. L.; Fox, D. J.; Keith, T.; Al-Laham, M. A.; Peng, C. Y.; Nanayakkara, A.; Gonzalez, C.; Challacombe, M.; Gill, P. M. W.; Johnson, B. G.; Chen, W.; Wong, M. W.; Andres, J. L.; Head-Gordon, M.; Replogle, E. S.; Pople, J. A. *Gaussian 98W*, version 5.2; Gaussian, Inc.: Pittsburgh, PA, 1998.

(15) Lehmann, K. K.; Scoles, G.; Pate, B. H. *Annu. Rev. Phys. Chem.* **1994**, *45*, 241.

(16) Nesbitt, D. J.; Field, R. W. *J. Phys. Chem.* **1996**, *100*, 12735.

(17) Kim, H. L.; Kulp, T. J.; McDonald, J. D. *J. Chem. Phys.* **1987**, *87*, 4376.

(18) Perturbations are, however, observed in the spectra of rotational levels of higher J and Ka (Rees, F. S.; Pate, B. H. Unpublished data).

(19) McIlroy, A.; Nesbitt, D. J. *J. Chem. Phys.* **1990**, *92*, 2229.

(20) Engelhardt, C.; Keske, J. C.; Rees, F. S.; Self-Medlin, Y. B.; Yoo, H. S.; Pate, B. H. *J. Phys. Chem. A* **2001**, *105*, 6800.

(21) This molecule was included in the analysis of the previous two papers of this series. As explained in this paper, vibrational relaxation rates of 4-fluorobutyne have been assigned to the trans conformation.

(22) Ruoff, R. S.; Klots, T. D.; Emilsson, T.; Gutowsky, H. S. *J. Chem. Phys.* **1990**, *93*, 3142.

(23) Fraser, G. T.; Suenram, R. D.; Lugez, C. L. *J. Phys. Chem. A* **2001**, *105*, 9859.

(24) Stuchebrukhov, A. A.; Marcus, R. A. *J. Chem. Phys.* **1993**, *98*, 6044.

(25) Stuchebrukhov, A. A.; Mehta, A.; Marcus, R. A. *J. Phys. Chem.* **1993**, *97*, 12491.

(26) Quack, M.; Stohner, J. *J. Phys. Chem.* **1993**, *97*, 12574.

(27) Gruebele, M.; Bigwood, R. *Int. Rev. Phys. Chem.* **1998**, *17*, 91.

(28) Another possible reason for this discrepancy is that the molecular-beam measurements for these two systems are the highest signal-to-noise measurements that we have achieved. As discussed in the text, higher sensitivity makes it possible to measure more transitions far from the central frequency, and this leads to the determination of faster IVR rates (compared to those obtained from lower-sensitivity measurements).

(29) Fraser, G. T.; Pate, B. H.; Bethardy, G. A.; Perry, D. S. *Chem. Phys.* **1993**, *175*, 223.

(30) Laenen, R.; Rauscher, C. *Chem. Phys. Lett.* **1997**, *274*, 63.

(31) Self-Medlin, Y. B.; Yoo, H. S.; Pate, B. H. Unpublished data.

(32) Jona, P.; Gussoni, M.; Zerbi, G. *J. Phys. Chem.* **1981**, *85*, 2210.

(33) Nyquist, R. A.; Potts, W. J. *Spectrochim. Acta* **1960**, *16*, 419.

(34) Evans, J. C.; Nyquist, R. A. *Spectrochm. Acta* **1963**, *19*, 1153.

(35) Grote, R. F.; van der Zwan, G.; Hynes, J. T. *J. Phys. Chem.* **1984**, *88*, 4676.

(36) Egorov, S. A.; Skinner, J. L. *J. Chem. Phys.* **1996**, *105*, 7047.

(37) Stratt, R. M.; Maroncelli, M. *J. Phys. Chem.* **1996**, *100*, 12981.